Mesoscale x-ray diffraction measurement of stress relaxation associated with buckling in compressed thin films

Philippe Goudeau[a] and Pascale Villain
Laboratoire de Métallurgie Physique, UMR 6630 CNRS, Université de Poitiers, SP2MI, Bvd Marie et Pierre Curie, 86962 Futuroscope Chasseneuil, France

Nobumichi Tamura and Howard A. Padmore
Lawrence Berkeley National Laboratory, 1 Cyclotron Road, Berkeley, California 94720

(Received 28 November 2002; accepted 15 May 2003)

Compressed thin films deposited on substrates may buckle depending on the geometrical and mechanical properties of the film/substrate set. Until recently, the small dimensions of the buckling have prevented measurements of their local in plane internal stress distribution. Using a scanning x-ray microdiffraction technique developed at a third generation x-ray synchrotron source, we obtained thin film internal stress maps for circular blisters and telephone chord buckling with micrometric spatial resolution. A fair agreement was found between the film delamination topology observed by optical microscopy and the measured stress maps. We evidenced residual stress relaxation associated with the film buckling: the top is essentially stress free while adherent region exhibits large compressive stresses. © *2003 American Institute of Physics.*
[DOI: 10.1063/1.1591081]

Thin films are used in many technological areas such as microelectronics and bio medical applications (implants), involving small dimensional devices, called microelectromechanical systems. Their reliability is principally dependent on the mechanical stability of the film/substrate set and thus on the intrinsic mechanical and adhesion properties of the film.

Physical vapor deposition techniques are widely used in related industries and resulting thin films bonded on nonepitaxial substrates generally exhibit large residual stresses due to the mismatch between the film and the substrate. Their structure, morphology—grain size and stress state are tightly controlled by the deposited atom energy. For instance, ion beam sputtering induces nanometric grain sizes, strong compressive residual stresses, and a large amount of unit cell defects. A compressive in plane stress can spontaneously lead the film to buckle in order to relieve this stress; this phenomenon generally happens when the film deposited under vacuum is submitted to the atmospheric pressure outside the deposition chamber. Buckling patterns could have a simple shape like circular blisters (Ni or Au on Si) or more complex ones like ''telephone chord'' wrinkles. These effects are undesirable and much effort was undertaken to theoretically study these phenomena by way of modeling and simulation.[1–6]

The buckling phenomenon is unambiguously attributed to a relaxation of the elastic energy stored in the film. However, the small dimensions of the buckling have so far prevented one from obtaining direct strain/stress measurements at the buckling location to support these theoretical results. Techniques like wafer curvature are used to measure the overall average stress in these films, but do not have the spatial resolution needed to map strain/stress on and around a buckling.[7] The micro-Raman technique may be applied for stress mapping at a micron scale and recent works have illustrated its potentialities in epitaxial lateral overgrown (ELO) GaN on Si substrates[8] or around a microindentation on Si.[9] Another suitable nondestructive optical microprobe technique based on Cr^{3+} piezospectroscopy has also been applied for residual stress mapping in alumina films formed by oxidation of alumina-forming alloys.[10,11] However, these techniques may only be considered for specific materials such as ceramics, oxides and semiconductors with well-defined microstructure and thus does not hold for pure metals.

In this work, we apply a scanning x-ray microdiffraction (μSXRD) technique capable of resolving stress variations at micron level in nanocrystalline samples.[12] This technique takes advantage of x-ray focusing optics at synchrotron sources of third generation, allowing one to obtain micron to submicron size intense x-ray probes, large area charge coupled device (CCD) technology, and analytical methods for fast data collection and reduction with no required sample or detector rotation.

Investigated samples are 630 nm Au and 300 nm W polycrystalline thin films deposited at room temperature by ion beam sputtering technique on a 650-μm-thick (100) Si wafer covered with native oxide. Details concerning sample preparation may be found in Ref. 13. An estimate of the total stress value in Au and W films has been obtained by measuring the three-dimensional buckling dimension or by applying the curvature method using a thinner substrate of the same nature such as Si (100) wafer, for instance, with a specific geometry which may prevent thin film buckling.[7] The average stress value is about -350 ± 80 MPa for gold films and -3.0 ± 0.4 GPa for W films.

The x-ray microdiffraction beamline setting at the Advanced Light Source has been described in detail elsewhere.[12,14] The instrument is capable of achieving an x-ray spot size on the sample of 1 μm^2 by using a pair of elliptically bent Kirkpatrick–Baez focusing mirrors and was

[a]Author to whom correspondence should be addressed; electronic mail: philippe.goudeau@univ-poitiers.fr

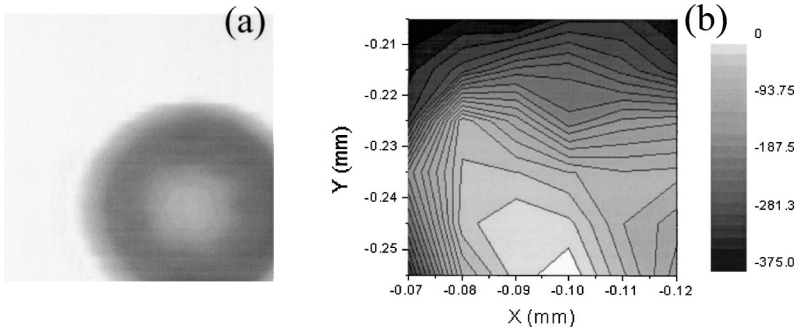

FIG. 1. (a) Optical microscope image of an approximately 54-μm-diam blister in a 630 nm thin Au film deposited on Si. (b) Corresponding stress map obtained by μSXRD. The stress intensity scale is expressed in MPa units.

designed for white beam as well as for monochromatic beam microdiffraction experiments. Monochromatic beam with energy ranging from 5.5 to 14 keV is obtained by inserting a four-crystal (111) Si monochromator in the path of the white beam. One characteristic of this design is that the white and the monochromatic beam paths are colinear allowing for the illumination of the sample with either type of radiation at the same exact location. The sample sits on an XYZ Huber stage and can therefore be raster scanned under the x-ray microbeam. At each step, a diffraction pattern is collected via a 9×9 cm area CCD detector. A Ge solid state detector coupled to a multichannel analyzer is also used to collect fluorescence signal.

In the thin films, buckling is first identified using an optical microscope and its positions are precisely measured with respect to a visible reference position also identifiable by x-ray microfluorescence. We chose a step corner realized during the deposition process with a thin silicon mask. This allows one to precisely locate the region of interest with the x-ray microbeam. Buckles are then scanned using a 10–15 μm step size and a typical 3×3 μm^2 x-ray spot size on the sample surface; at each step a diffraction pattern is collected with the CCD camera. Geometrical parameters (radial and angular positions of the CCD detector with respect to the incoming beam direction and the illuminated area on the sample) are determined by taking a white beam diffraction pattern of the Si single crystal substrate. A custom software rapidly indexes the Si pattern and provides the required calibration parameters by nonlinear least square fitting.

The grain size (<10 nm) being typically much smaller than the beam size for all samples, the CCD frame yields a ''powder''-type ring with monochromatic beam. CCD diffraction patterns were taken in reflection mode, with the sample making an angle of 45° with respect to the incoming x-ray beam and the CCD on a vertical slide at about 35 mm above the point of impact in the sample. The intensity distributions on the rings are consistent with a preferential $\langle 111\rangle$ and $\langle 110\rangle$ fiber texture for gold and tungsten, respectively.

Residual stresses within a sample can be determined by measuring the induced change in lattice constant with x rays. The analysis of the diffraction patterns consists in applying the ''d vs $\sin^2\Psi$'' technique[15,16] to the rings, where ψ is the angle between the surface normal and the normal to the diffracting planes. Indeed, each point on a given ring corresponds to a different ψ value. For that purpose, knowing the geometrical calibration parameters and the direction of the surface normal, the CCD diffraction pattern is converted into a $2\theta-\psi$ frame.

With the assumption that the average stress under the area illuminated by the x-ray beam is biaxial ($\sigma_{xx}=\sigma_{yy}=\sigma$) with no σ_{xy} shear component, we have the classical ''d'' vs $\sin^2\Psi$ relation

$$(d-d_0)/d_0=\{(1+\nu)/E\}\sigma\sin^2\Psi-\{2\nu/E\}\sigma, \tag{1}$$

where E is the Young's modulus and ν the Poisson's ratio of the material. The stress σ is then calculated using the slope determined from the d vs $\sin^2\Psi$ plot. For a textured film, E and ν are replaced by expressions which are function of their elastic compliances values S_{nn}. For instance, for an $\langle 111\rangle$ uniaxially textured face centered cubic structure (Au), the d vs $\sin^2\Psi$ relation becomes

$$(d-d_0)/d_0=\{S_{44}/2\}\sigma\sin^2\Psi-\{(2S_{11}+4S_{12}-S_{44})/3\}\sigma. \tag{2}$$

This formalism has been applied in first approximation for analyzing our x-ray diffraction data. It allows one to get in a simple way the average in depth residual stress state in the film and to follow its evolution over the buckling. One may keep in mind that the stress value is dependent on the direction of x-ray which is the y-scan axis in our case. This consideration is important in the case of tungsten films because the stress state in the wrinkles along principal in plane directions is not isotropic ($\sigma_{xx}\neq\sigma_{yy}$). Concerning the reliability of our stress mapping, we assume that the surface curvature does not affect the precision on stress measurement. Indeed, the radius of surface curvature (for instance, 135 μm in Au film blisters) is much larger than the x-ray spot size (3×3 μm^2).[17] On the contrary, the variation of the normal to the sample surface during the buckling scan may sensibly influence the stress value.[18] For instance, a maximum deviation of 12° may be expected for a Au blister with a width of 54 μm and a height of 2.7 μm. It corresponds to x-ray measurements done at the frontier zone between adherent and buckle film regions. Of course, this angle is nil at the top of the buckling. In order to appreciate the normal rotation effect, we calculated the resulting maximum variation for the stress in the case of gold buckling; a magnitude decrease of about 15% is expected, the stress sign remaining the same. The stress is then overestimated at the beginning of the relaxation profile (frontier zone). Independent of this geometrical effect, an extension of the ψ-angular domain of measurement would also greatly increase the precision on stress determination.

Figure 1(b) shows the output of a μSXRD scan performed over a circular blister (diameter=54 μm) of a 630-nm-thick Au film on Si [Fig. 1(a)]. The scan over the blister was performed in 10 μm step using a 300 s exposure time and a monochromator energy of 6 keV ($\lambda=0.2066$ nm). The stress map shows that the stress in the adherent film in the

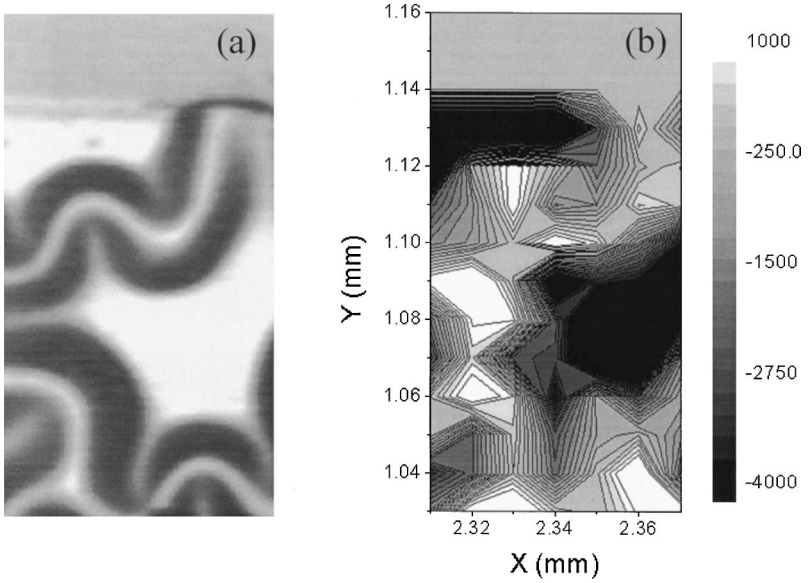

FIG. 2. (a) Optical microscope image of wrinkled regions close to a step in a 300 nm thin W film deposited on Si. (b) Corresponding stress map obtained by μSXRD. The stress intensity scale is expressed in MPa units.

vicinity of the blister is about −400 MPa while it vanishes to around 0 MPa in the middle of it.

Figure 2(b) shows the stress map as a result over a 60 μm×140 μm area of buckling on a 300-nm-thick W film on Si [Fig. 2(a)]. The μSXRD scan was performed with a 10 μm step size, with an exposure time of 600 s and a monochromator energy of 7.5 keV (λ=0.165 315 nm). A fair agreement is found between the film delamination topology observed by optical microscopy and the measured x-ray stress maps. However, one may keep in mind that optical and x-ray observations are done in a different way: normal to the film surface for the first and 45° inclination of the sample surface for the second.

The measured stress values in the adherent regions are higher than the average stress obtained from wafer curvature techniques. This might be due to in plane stress heterogeneity and also to the fact that we were using elastic constant values of bulk. Recent studies have shown that thin film values may differ from the bulk ones[19,20] because of their particular microstructure; a strong softening of the Young modulus in stainless steel films has been measured.[21] A similar effect may be expected in our Au and W films produced by ion beam sputtering. This would contribute to scale down the x-ray measured values to the wafer curvature measurements.

Stress mapping measurements on thin film buckling at a tenth micrometer scale have been successfully achieved. A nearly stress-free state is measured at the top of the buckling in two different nanocrystalline materials and blister geometry, whereas adherent regions are strongly compressed. Topology of film delamination areas observed by optical microscopy and the measured x-ray stress maps is similar. More precise x-ray measurements are engaged as well as finite element calculations of the stress field associated with two-dimensional blisters and wrinkles in these metallic thin films. In particular, the existence of a strain/stress gradient through the film thickness due to its bending has to be considered for the x-ray data analysis.[15,16,22] Confrontation of the stress profiles will permit precise boundary conditions of the model and thus will lead to a better understanding of relevant parameters controlling thin film buckling.

The Advanced Light Source is supported by the Director, Office of Science, Office of Basic Energy Sciences, Materials Sciences Division, of the U.S. Department of Energy under Contract No. DE-AC03-76SF00098 at Lawrence Berkeley National Laboratory. The authors thank R. S. Celestre and W. A. Caldwell from the Advanced Light Source, Berkeley, for their technical assistance at the beam line.

[1] G. Gioia and M. Ortiz, Adv. Appl. Mech. **33**, 119 (1997).
[2] B. Audoly, Phys. Rev. Lett. **83**, 4124 (1999).
[3] P. Peyla, Phys. Rev. E **62**, R1501 (2000).
[4] M. George, C. Coupeau, J. Colin, F. Cleymand, and J. Grilhé, Philos. Mag. A **82**, 633 (2002).
[5] N. Sridhar, D. J. Srolovitz, and B. N. Cox, Acta Mater. **50**, 2547 (2002).
[6] M. W. Moon, H. M. Jensen, J. W. Hutchinson, K. H. Oh, and A. G. Evans, J. Mech. Phys. Solids **50**, 2355 (2002).
[7] D. W. Zheng, X. H. Wang, K. Shyu, C. Chen, C.-T. Chang, K. N. Tu, A. K. Mal, and Y. F. Guo, J. Mater. Res. **17**, 1795 (2002).
[8] M. Benyoucef, M. Kuball, B. Beaumont, and P. Gibart, Appl. Phys. Lett. **80**, 2275 (2002).
[9] P. Puech, S. Pinel, R. G. Jasinevicius, and P. S. Pinazi, J. Appl. Phys. **88**, 4582 (2000).
[10] D. M. Lipkin and D. R. Clarke, Oxid. Met. **45**, 267 (1996).
[11] A. Atkinson, D. R. Clarke, and S. J. Webb, Mater. Sci. Technol. **14**, 531 (1998).
[12] A. A. MacDowell, R. S. Celestre, N. Tamura, R. Spolenak, B. Valek, W. L. Brown, J. C. Bravman, H. A. Padmore, B. W. Batterman, and J. R. Patel, Nucl. Instrum. Methods Phys. Res. A **467,468**, 936 (2001).
[13] P. Goudeau, P. Villain, P.-O. Renault, N. Tamura, R. S. Celestre, and H. Padmore, Mater. Sci. Forum **404–407**, 709 (2002).
[14] N. Tamura, R. S. Celestre, A. A. MacDowell, H. A. Padmore, R. Spolenak, B. C. Valek, N. Meier Chang, A. Manceau, and J. R. Patel, Rev. Sci. Instrum. **73**, 1369 (2002).
[15] I. C. Noyan and J. B. Cohen, *Residual Stress Measurement by Diffraction and Interpretation* (Springer, New York, 1987).
[16] V. Hauk, *Structural and Residual Stress Analysis by Non Destructive Methods: Evaluation Application, Assessment* (Elsevier, Amsterdam, 1997).
[17] B. Dionnet, M. François, J.-M. Sprauel, and F. Nardou, J. Appl. Crystallogr. **32**, 883 (1999).
[18] J. Matejicek and S. Sampath, Acta Mater. **49**, 1993 (2001).
[19] A. J. Kallman, A. H. Verbruggen, and G. C. A. M. Janssen, Appl. Phys. Lett. **78**, 2673 (2001).
[20] K. F. Badawi, P. Villain, P. Goudeau, and P.-O. Renault, Appl. Phys. Lett. **80**, 4705 (2002).
[21] P. Goudeau, P.-O. Renault, P. Villain, C. Coupeau, V. Pelosin, B. Boubeker, and K. F. Badawi, Thin Solid Films **398,399**, 496 (2001).
[22] M. Leoni, U. Welzel, P. Lamparter, E. J. Mittemeijer, and J. D. Kamminga, Philos. Mag. A **81**, 529 (2001).